Role of tidal range and coastline morphology on the evolution of two macrotidal sand spits

Bernadette Tessier, Clément Poirier, Mikkel Fruergaard, Eric Chaumillon, Pierre Weill, X. Bertin, Dominique Mouazé

Received: 12 May 2023 | Revised: 27 June 2024 | Accepted: 8 July 2024

DOI: 10.1002/dep2.304

The Depositional Record
Open Access
A journal of the International Association of Sedimentologists
IAS
WILEY

ORIGINAL RESEARCH ARTICLE

Role of tidal range and coastline morphology on the evolution of two macrotidal sand spits

Bernadette Tessier[1] | **Clément Poirier**[1] | **Mikkel Fruergaard**[2] | **Eric Chaumillon**[3] | **Pierre Weill**[1] | **Xavier Bertin**[3] | **Dominique Mouazé**[1]

[1]Université de Caen Normandie, CNRS, Univ Rouen, Normandie Univ, UMR 6143 M2C, Caen, France

[2]Department of Geosciences and Natural Resource Management (IGN), University of Copenhagen, Copenhagen K, Denmark

[3]UMR 7266 LIENSs, CNRS-La Rochelle Université, La Rochelle, France

Correspondence
Bernadette Tessier, Université de Caen Normandie, CNRS, Univ Rouen, Normandie Univ, UMR 6143 M2C, 24 rue des Tilleuls, Caen, 14000, France.
Email: bernadette.tessier@unicaen.fr

Funding information
French Ministry of Environment (Ministère de l'Ecologie, du Développement Durable et de l'Energie, MEDDE), Grant/Award Number: BLiNiS research project (2013-2015); Carlsberg Foundation, Denmark, COASTEVENT, Grant/Award Number: CF14-0173 and CF15-0254

Abstract

The present study examines the stratigraphy of two sandspits that both appeared and developed since the middle of the 17th century during the Little Ice Age. The Arçay spit is located along the macrotidal Atlantic coast in South-West France with a maximum tidal range of 6.5 m. The Pointe du Banc in the English Channel, North-West France, is located in a hypertidal coastal setting with a tidal range of up to 14 m. The evolution of the two spit systems has been compared using historical maps, ground penetrating radar data and facies analysis and geochronological data from sediment cores. The Pointe du Banc spit developed between 1650 and 1750 CE, in a dominant seaward direction while the main mode of construction of the Arçay spit was in a longshore direction. It is proposed that this difference relates to sediment supply and coastline morphology. At the Pointe du Banc spit, the large tidal range causes a long wind fetch and sustained aeolian sediment supply. Moreover, the spit is located at the apex of a large-scale embayment where sediment transport from north and south converges. Combined, these factors result in a positive sediment budget and seaward shoreline progradation. At the Arçay spit, high wave obliquity results in a large littoral drift and sustained longshore spit construction. At both locations, low gradient shorefaces may have favoured a net landward-directed sediment flux that supply sand to the foreshore.

KEYWORDS

aeolian fetch, coastal barrier, longshore transport, sediment supply, stratigraphy, tidal range

1 | INTRODUCTION

Coastal barriers, including sand spits, make up 6%–15% of the world's coastlines (Stutz & Pilkey, 2011). Coastal barriers are critical in providing natural protection against the waves of the open ocean, for ecosystems of back-barrier and lagoon environments, including coastal marshes and lowlands. Moreover, many coastal barriers often provide high recreational and economical value, and they can be densely populated (Zhang & Leatherman, 2011). Coastal barriers are dynamic systems prone to sediment reworking under the impact of storm waves that can cause

erosion, breaching and submersion (Masselink & van Heteren, 2014; Chaumillon et al., 2017). The Xynthia storm in February 2010, which hit the Vendée and Charente coasts in South-West France caused severe coastal erosion with breaching, overtopping and inundation of low-elevation coastal areas (Bertin et al., 2014). In the future, sea-level rise, and a likely increase in the frequency and intensity of storms (Nicholls & Cazenave, 2011; Oppenheimer et al., 2019; Easterling et al., 2000; Dobrynin et al., 2012; Vousdoukas et al., 2016), may result in more marine flooding events that threaten the increasing number of people living along the coast (McGranahan et al., 2007).

During the Mid to Late Holocene, that is, since approximately 6500 years ago, many coastal barriers started to form along the North-West European coasts. The evolution of the coastal landscapes was influenced by cyclic climate oscillations with a periodicity of around 1500 years and recurrence of colder and enhanced stormy periods (Sorrel et al., 2012). The impacts of these stormy and windy climate phases are recorded in deposits along the coasts of Western Europe (Sorrel et al., 2012; van Vliet-Lanoë et al., 2014a, 2014b; Zazo et al., 2008; Allard et al., 2009; Clarke & Rendell, 2011; Sabatier et al., 2012). The greater wind intensity during these periods resulted in enhanced aeolian transport that contributed to the formation of dune belts (Jackson et al., 2005; Clarke & Rendell, 2011; Costas et al., 2012, 2016), breaching of coastal barriers (Jelgersma et al., 1995; Billeaud et al., 2009; Tessier et al., 2010; Sabatier et al., 2012) and more frequent flooding of back-barrier marshes (Spencer et al., 1998; Billeaud et al., 2009). The last of these stormy and windy phases coincides with the Little Ice Age (LIA) which lasted from about 1350–1850 CE (cf. Miller et al., 2012).

Along the French mesotidal to hypertidal coasts of the English Channel and the Atlantic Ocean, the evolution of coastal barriers is also influenced by the tidal regime. The nodal lunar cycle with a period of 18.61 years and the perigean lunar cycle with a period of 8.85 years influence the impact of extreme water levels (Menendez & Woodworth, 2010). Studies on the shelly chenier barriers located in the south of the bay of Mont-Saint-Michel showed that variations in the mean sea level modulated by nodal or perigean cycles constitute a key factor controlling the morphodynamic behaviour of these barriers at a multidecadal time scale (Weill, 2010; Weill et al., 2012; Tessier et al., 2019).

Several studies providing sedimentological and geochronological data have shown that widespread formation of wave and wind-built barriers occurred along the western coasts of Europe from *ca* 1500 to 1900 CE under the intense wind and wave climates of the LIA (Poirier et al., 2017a; Jackson et al., 2019). Presented here is a comparative study of the Arçay (ARC) and Pointe du Banc (PDB) spits located along the coasts of the Atlantic Ocean in South-West France and the English Channel in North-West France, respectively. Detailed studies on the stratigraphy, morphology and evolution of the two spits have been published in Poirier et al. (2017a, 2017b) and Fruergaard et al. (2020). Both spits are wave-dominated and started to form during the LIA but while the ARC spit developed under macrotidal conditions with a tidal range up to 6.5 m the PDB spit developed under hypertidal conditions with a tidal range up to 14 m. The comparison of the spits mainly focuses on stratigraphic aspects, i.e. the internal architecture and chronology, featuring the evolution and depositional mode of the two spits. The aim of the study is to evaluate the effect of the tidal range and coastal morphology on the construction of wave-dominated and tide-influenced coastal bodies. Only a few studies have investigated the effect of the tidal range on the evolution of coastal barriers and spits. Hayes (1979) established the relationships between tidal range and the morphology of coastal barriers, which developed in micro-tidal to meso-tidal settings along the eastern coast of the United States. Mulhern et al. (2017) highlighted that these relationships were not straightforward, especially for mixed tide and wave-influenced settings. Although the studies of Hayes (1979) and Mulhern et al. (2017) focus on barrier islands and not barrier spits these works demonstrated that the impact of the tidal context on barrier evolution is difficult to constrain. It is well-documented that the tidal context is important in spit terminus dynamics with tidal currents overprinting wave-driven sedimentation (Fruergaard et al., 2020). The role of waves is modulated by tidal range, which directly affects wave-induced longshore currents and consequently spit morphology. This effect is well-illustrated by Robin et al. (2020) along the hypertidal coast of North-West France. Dashtgard and Gingras (2007) provided a list of sedimentological and morphological indicators of tidal influence for coarse-grained barriers that could be deciphered in the barrier architecture. These architectural characteristics included the thickness of the barrier succession and the occurrence of a steep beachface above a gentle sloping low-tide terrace. However, other studies of hypertidal coasts showed that these criteria are not unambiguous (Montes et al., 2018; Pancrazzi et al., 2022). The present study highlights a significant difference in the dynamics and patterns of evolution between the two investigated spits. It is suggested here that tidal range is one of the main-controlling factors in spit evolution because it causes differences in wind-induced sediment availability. The larger tidal range in hypertidal settings likely favours a relatively more positive sediment budget and thus dominant seaward spit construction. In contrast,

relatively less aeolian sediment is sourced to spits in macrotidal settings, resulting in dominant down-drift elongation of the spit.

2 | THE PHYSICAL AND GEOLOGICAL SETTING OF THE STUDY SITES

The two sandspits were selected because they are exposed to different tidal ranges so that the role of tides versus wave climate in their evolution can be compared.

2.1 | The PDB sandspit (English Channel)

The PDB spit is located along the coast of the Normandy-Brittany Gulf in the English Channel. It is part of a regional set of sand spits along the west coast of the Cotentin Peninsula, from Granville to Barneville-Carteret (Figure 1A through D). It is located at the entrance to the Ay estuary, named the 'Havre de Lessay'. The River Ay has a length of 33 km and a catchment area of 170 km^2. The mean water discharge in the river does not exceed 0.1 $m^3 s^{-1}$, reaching up to 0.7 $m^3 s^{-1}$ during flood periods (HydroPortail, station I6983010). The PDB spit is triangular shaped with a length of about 3 km and a width at its proximal end up to 2.5 km. The spit is oriented along a NNW–SSE axis, with its distal end towards the south. The spit is exposed to a hypertidal, semidiurnal tide with a tidal range up to about 14 m during the highest spring tides (hypertidal B and C types according to Archer, 2013). The tidal current velocity reaches up to 1 $m s^{-1}$ offshore of the west coast of the Cotentin Peninsula and up to 3 $m s^{-1}$ in the mouth of the estuary (Levoy et al., 2000). Dominant winds are from the south-west and north-west and the strongest winds come from the west and north-west directions during the winter. With respect to wave dynamics, the PDB spit area is a low-energy coastline due to the shallow bathymetry of the Normandy-Brittany Gulf and the lee-effect generated by the Channel Islands and various shoals and islets (Figure 1B). The annual mean significant offshore wave height is less than 0.5 m (Robin et al., 2020) but during storms, waves and swells may increase considerably. The maximum annual significant wave height offshore of Barneville-Carteret is about 4.2 m, decreasing to about 2.8 m offshore of Granville (Levoy et al., 2000).

Most works along the west coast of the Cotentin Peninsula dealing with sedimentology, focussed on the recent morphodynamics of the Pointe d'Agon (Agon spit), located 25 km south of the PDB spit (Figure 1B), at the entrance of the Sienne Estuary (Robin & Levoy, 2007; Robin et al., 2007, 2009a, 2009b, 2020; Levoy et al., 2013; Montreuil et al., 2014). At the regional scale, Haslett et al. (2003) evaluated the rate of salt-marsh growth since the end of the 19th century into several of the estuaries including the 'Havre de Lessay'. According to Schwartz (1982), the PDB spit can be classified as a simple spit that formed by the accretion of aeolian dune ridges and berms on top of a dissipative beach (tidal flat; model C in Tamura, 2012). The dune ridges are visible on the high-resolution digital terrain model of the area (Figure 1D). The PDB spit was selected for the present comparative study due to the hypertidal coastal context and the limited coastal management in the area.

The stratigraphy, architecture and absolute chronology of the PDB spit was investigated in Fruergaard et al. (2020). The main conclusions of this study are: (1) the spit has a complex sedimentary architecture made of wave-dominated and tide-dominated sedimentary bodies; (2) its progradation induced by littoral drift is the main process for spit elongation; (3) the spit terminus grows in height and width due to sediment convergence caused by landward migration of swash bars and seaward migration of tidal dunes; (4) the long-term accretion rates varied considerably in response to changes in sediment supply; (5) variations in storminess together with the large-scale topography of the coast controlled the sediment supply and thus the evolution of the barrier system during the latest Holocene.

2.2 | The Arçay sandspit (Atlantic coast)

The ARC sandspit is located on the coast of the Bay of Biscay, in the inner part of the Pertuis Breton, which is a mixed tide-wave dominated, drowned incised valley (Chaumillon et al., 2008; Figure 1A,E–G). The ARC spit constitutes part of the mouth of the River Lay, a small river (length: 119 km; catchment surface: 1980 km^2) with mean water discharge up to 5 $m^3 s^{-1}$, reaching up 150 $m^3 s^{-1}$ during floods (*HydroPortail*, station N3511610). The ARC spit is approximately 11 km long, 1.2 km wide, and is oriented along a NW–SE axis, with its terminus towards the south-east. The tidal regime is semi-diurnal and ranges between 1.1 (neap tides) and 6.5 m (spring tides). The velocity of tidal currents along the ARC marine foreshore typically vary between 0.1 and 0.3 $m s^{-1}$ (Dehouck et al., 2013). The offshore wave climate (60% of the time) is characterised by significant wave height between 1 and 2 m, a period ranging from 8 to 12 s, and waves approaching the shore from west-southwest to north-west directions (Bertin et al., 2008). Winter storms can episodically produce waves higher than 9 m (Bertin et al., 2013). Due to the presence of a shallow and extended shoreface (at low tide, the 10 m

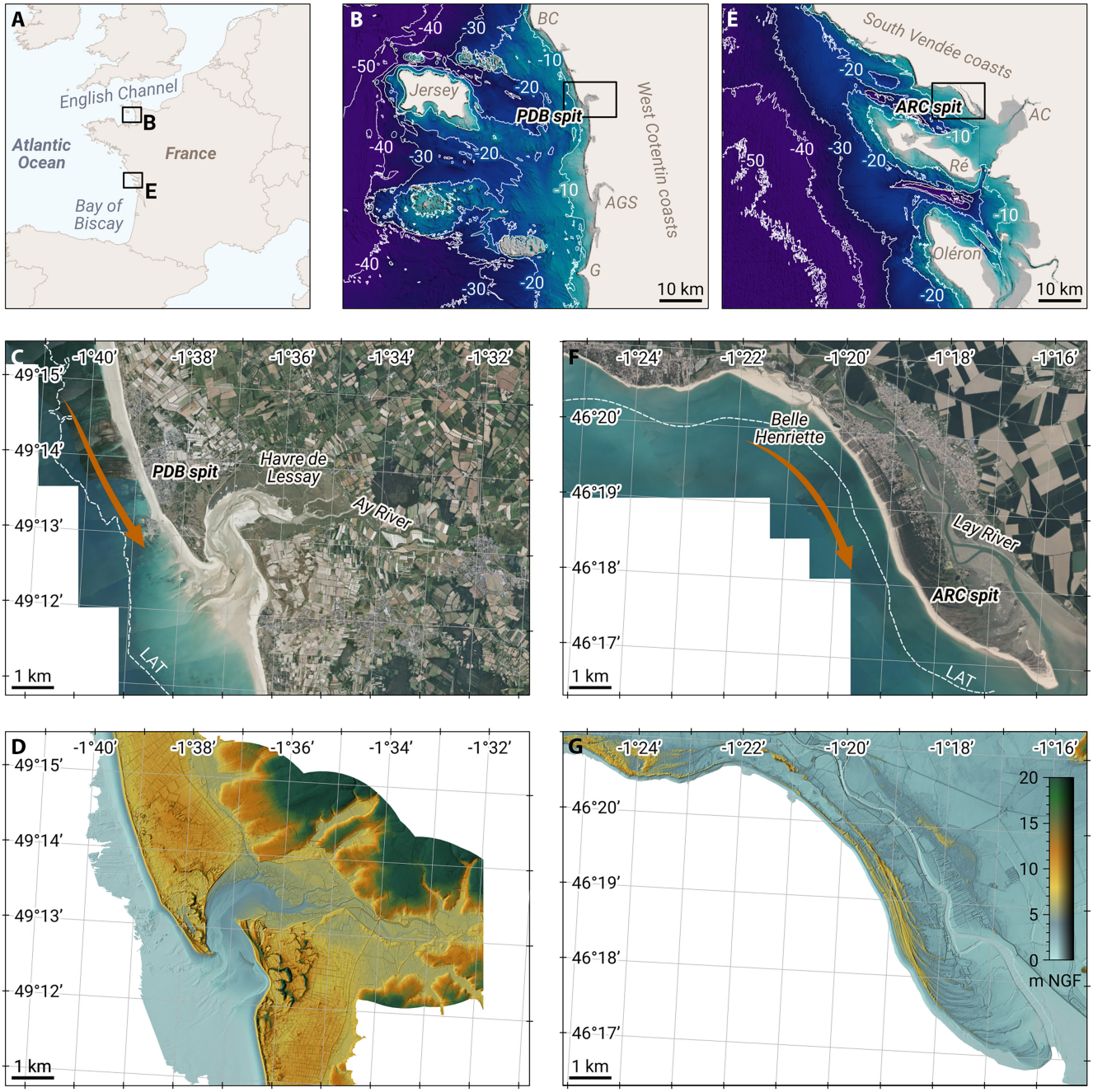

FIGURE 1 (A) General location map. (B, C, D) The Saint Germain-sur-Ay (PDB) sandspit, located along the hypertidal English Channel south coast in North-West France, where the tidal range is up to 14 m. (B) General location and bathymetric map with 10 m contour lines (SHOM, 2015). BC, Barneville-Carteret rocky cape; G, Granville rocky cape; AGS, Agon spit. (C) Close up view of the PDB spit (IGN aerial image). (D) PDB spit high-resolution Digital Terrain Model (IGN Litto3D). (E–G) The Arçay (ARC) sandspit, located along the macrotidal Bay of Biscay coast of West France, where the tidal range is up to 6.5 m. (E) General location and bathymetric map with 10 m contour lines (SHOM, 2015). AC, Aiguillon cove. (F) Close up view of the ARC spit (IGN aerial image). (G) ARC spit high-resolution Digital Terrain Model (IGN Litto3D). For easier comparison, panels (B) and (E), panels (D) and (G) share the same extent and colour scales. Panels (C) and (D) and Panels (F) and (G) share the same extent. Bathymetric and topographic data are expressed in metres NGF.

water-depth isoline is found about 10 km offshore), wave energy is attenuated when reaching the shoreline (Bertin et al., 2007; Allard et al., 2008; Lashley et al., 2019) and the dominant wave direction is restricted to the west or west-southwest (Allard et al., 2008). The ARC spit has been the subject of several studies on its morphological and sedimentary evolution (Beigbeder & Verger, 1967; Auphan & Verger, 1969; Galichon, 1984; Deat, 1995; Bertin et al., 2007; Allard, 2008; Allard et al., 2008; Bertin et al., 2008; Musereau, 2009; Poirier et al., 2017a, 2017b).

It is a compound spit (Schwartz, 1982) formed by welding of swash bars that eventually merge into hook-shaped supratidal berm ridges topped by aeolian deposits (model D in Tamura, 2012). The hooks are visible on the digital terrain model (DTM) of the area (Figure 1G).

Based on a comparison between SPOT satellite images and a high-resolution wave hindcast, Allard et al. (2008) suggested that rhythmic ridge-swale successions from 1987 to 2005 CE were controlled by wave-height variability. Under large waves, the divergence of the longshore transport is strongest around the fulcrum point, which promotes spit elongation towards the south-east, whereas under moderate waves, longshore transport decreases along the spit which promotes berm ridge curvature towards the east.

Poirier et al. (2017b) reconstructed the ARC spit shoreline dynamics using historical maps and aerial photographs. The study showed that the rate of elongation was near-constant between 1675 and 2010 CE, with an average value of about 23 m year^{-1}. However, three distinct periods of increased elongation rates were identified lasting from 1811 to 1824 CE, 1909 to 1923 CE and 1984 to 1994 CE. These periods were characterised by positive North Atlantic Oscillation (NAO) and negative East Atlantic–West Russia (EA–WR) atmospheric circulation patterns. Such conditions are proxies of higher offshore and nearshore wave height, increasing longshore sediment transport. In a study of climate control on late Holocene high-energy sedimentation along coasts of the North-East Atlantic Ocean, Poirier et al. (2017a) included ground penetrating radar (GPR), core and ^{14}C age data collected in the ARC spit in the frame of the present project. Based on these data it was suggested that the spit construction started during the LIA, arguing that the spit development did not result from episodic very high-energy storm events as shown by Fruergaard et al. (2013) from the Danish Wadden Sea coast, but rather from higher-than-average wave-induced sediment transport that allowed optimal preservation (Poirier et al., 2017a).

3 | DATABASE

The present study relies on two main datasets: (1) Recent and historical documents (topographic maps, aerial photographs and digital elevation models) to compare the evolution and morphology of the two spits. (2) The GPR data, complemented with facies analysis and geochronological information obtained from sediment cores to compare the main characteristics of their stratigraphy. Poirier et al. (2017b) provided an accurate analysis of historical maps and aerial photographs to study the evolution of the ARC spit. A similar analysis of the PDB spit was performed in this study so the evolution of the two spits could be compared. Similarly, an analysis of the stratigraphy of the ARC spit has been carried out and synthesised in this study to compare it with the main results of stratigraphic analysis provided by Fruergaard et al. (2020) on the PDB spit.

3.1 | Historical maps and aerial photographs

3.1.1 | Data sources

Most historical cartographic documents originate from: (1) the database of the National Library of France (BNF, gallica.bnf.fr). The collection includes a wide chronological period, with nautical charts from the 16th to the 18th century. (2) The National Geographic Institute (IGN) database (geoportail.gouv.fr). The collection includes the General Staff maps produced from the 19th century and sets of aerial photographs from 1945, and as far back as the period from 1920 to 1930 CE. (3) The departmental archives of Vendée and Charente-Maritime (ARC spit) and of La Manche (PDB spit). These archives include documents of variable nature, generally after the 18th century. In total, 46 old historical maps and 29 sets of aerial photographs were obtained for the ARC spit area (Poirier et al., 2017b), compared to, respectively, 24 and 18 for the PDB spit.

3.2 | Map processing

For georectification of the oldest documents, the reference used is the legal projection system RGF93-Lambert93. Reference points for georectification on the historical maps are, for instance, the circles and crosses symbolising parish churches. For the aerial photographs, the intersections of paths or roads, or the corners of some characteristic buildings (farms, sheds, etc.) were used. Position of reference objects were obtained from the most recent topographic databases available for the two study sites.

3.2.1 | Digitisation

Once the maps and photographs were georectified, the coastlines were digitised. According to information given on the historical maps, the coastline on most maps corresponds to the level of high spring tide. On aerial photographs of the ARC spit, this elevation corresponds to the transition between wet (dark) and dry (light) sand, from

the subtidal platform of the spit to the supratidal hooks covered by aeolian deposits (cf. Allard et al., 2008). For a more detailed description of the historical map processing, see Poirier et al. (2020).

3.3 | GPR data

Ground penetrating radar is a geophysical tool suitable for studying the internal architecture of coastal barriers composed of sand to gravel-sized sediment, in the upper intertidal to supratidal limit (Neal & Roberts, 2000; Weill et al., 2012; Pancrazzi et al., 2022; Fruergaard et al., 2020). For the present study a 400 MHz antenna fitted with a SIR 3000 acquisition unit from GSSI (Geophysical Survey Systems, Inc.) was used for the two spits. The GPR data were processed using custom scripts implemented in the software R by adapting part of the MATGPR code (Tzanis, 2006). The successive steps of signal processing included (1) an adjustment of the time-zero position; (2) a filter to extract background noise; (3) gain function to increase the contrast; (4) the creation of a 1D velocity model for time-to-depth conversion. Relative dielectric permittivities of 5 for unsaturated aeolian sand and 26 for water-saturated sand (Neal, 2004) were applied in the model. The transition between the saturated and unsaturated sediment corresponds to the top of the water table, the position of which was deduced from the water-level elevation in small ponds at the two sites; (5) a static migration of the elevation of each trace according to the topography extracted from the DTM of the area (IGN, RGE ALTI 1 m). Figure 2 summarises the GPR data collected on the two spits.

3.4 | Sediment core data

Coring was performed using a vibracorer from the M2C laboratory which allows for extraction of cores up to 8 m long. Core positions were chosen based on GPR data. Figure 2 indicates the location of the sediment cores retrieved from the two spits (nine cores in the PDB spit; five cores in the ARC spit).

All cores were qualitatively described at the M2C laboratory for sedimentary facies analysis (nature and sedimentary structures, bioturbation). Samples for ^{14}C dating mainly consisted of mollusc shells, which were chosen in accordance with ecological and taphonomic criteria (Poirier et al., 2010) to avoid reworked shells. A total of 43 samples were sent to the Poznan Radiocarbon Laboratory in Poland (eight for the ARC spit, Poirier et al., 2017a; 35 for the PDB spit, Fruergaard et al., 2020). Calibration was performed with Calib 7.0 software (Stuiver & Reimer, 1993) applying the Marine13 curve for calibration, with a regionally averaged DR (Marine Reservoir Correction Database, Queens University, Belfast) of -36 ± 40 years for ARC and -28 ± 96 years for PDB (Tisnérat-Laborde et al., 2010). A mixed model (Mixed Marine Northern Hemisphere) was used for peat samples. To supplement the ^{14}C chronology, 13 samples from the PDB spit cores were dated using optically stimulated luminescence (OSL) at the Nordic Laboratory for Luminescence Dating,

FIGURE 2 Location of GPR lines and cores acquired on the PDB spit (A) and the ARC spit (B). In blue, GPR lines shown on Figure 4.

Aarhus University, Denmark. The original OSL dataset is from Fruergaard et al. (2020).

4 | RESULTS

4.1 | Coastline evolution since the last centuries

Historical map analysis allowed for construction of a chronological framework and for a determination of the evolution of the coastline of the ARC and PDB spits during the last centuries.

4.1.1 | The PDB spit

The PDB spit is mentioned for the first time in the surveys carried out by the Chevalier de Clerville during the 1670s (Figure 3 top). Several other maps were produced during the late 17th century by Sainte-Colombe and Mariette de la Pagerie. The coastline is consistently drawn on these

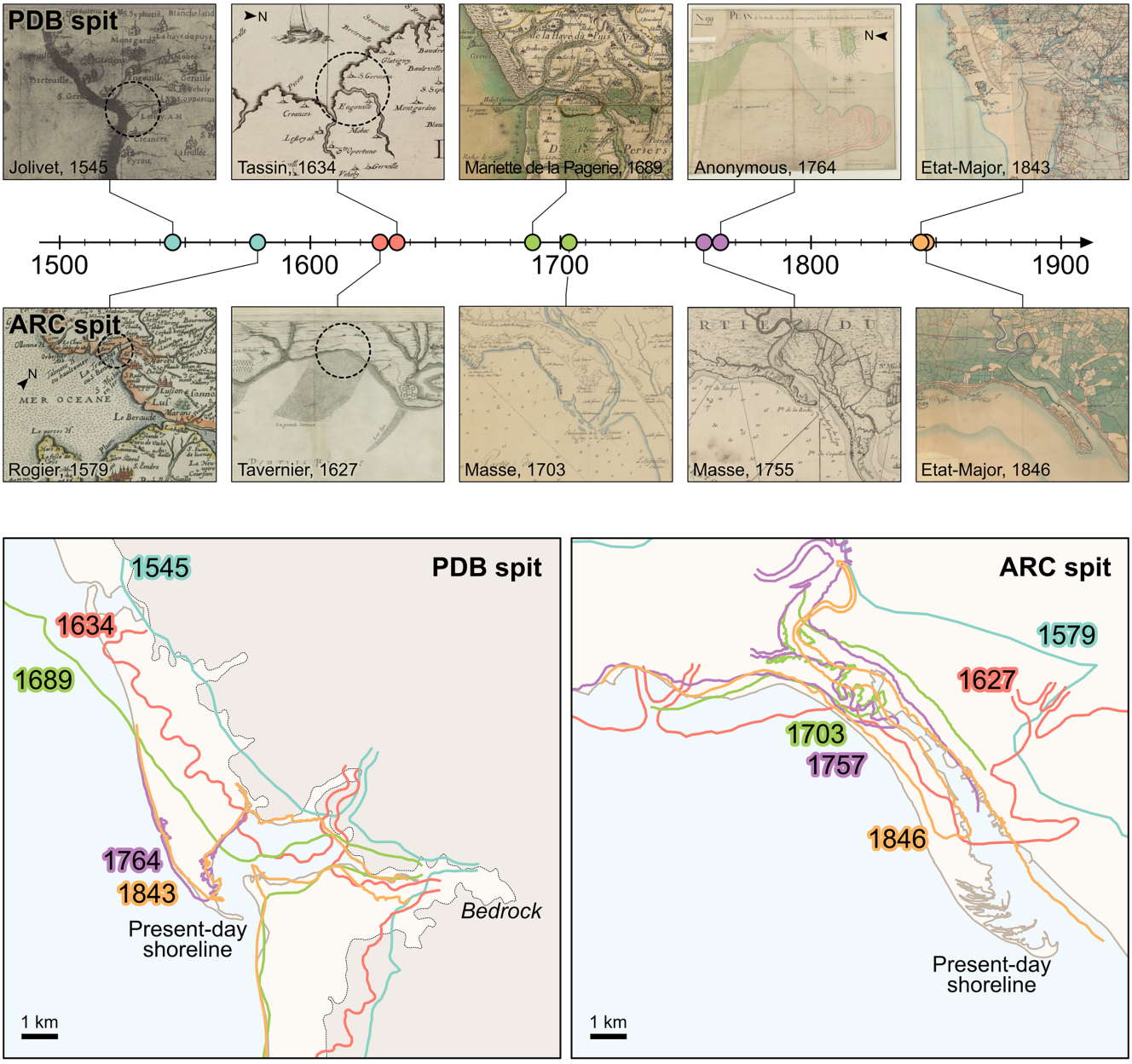

FIGURE 3 Comparison of coastline evolution of the PDB and ARC spit areas from the mid-16th century to the mid-19th century. Note the 1764 map of the PDB spit that has north oriented towards the left, while all other maps are oriented north upwards. Dashed circles indicate the approximate position of the spits on pre-16th century maps.

maps, all showing a wide-open estuary, oriented E–W, with a slightly recurved coastline at the location of the spit. This contrasts with the representation of Clerville in 1670 CE. The first reliable representation of the PDB spit dates back to 1764 CE. It indicates that the sandspit at this time had a shape and position almost identical to the present-day spit configuration.

4.1.2 | The ARC spit coastline evolution

Similarly to the PDB spit, the ARC spit appears for the first time on the topographic surveys of La Favolière, published in 1675 CE (Figure 3 bottom, after Poirier et al., 2017b). At this time, the spit was about 2–3 km long (the present-day spit is approximately 11 km long) and was composed of two to three hooks. The evolution of the spit is described by Poirier et al. (2017b) and by Allard et al. (2008) showing that the spit regularly elongated until today. Note that on the 1627 CE map (Tavernier map), the drawn spit is not the ARC spit but its predecessor, the Aiguillon spit, which was active before the formation of the ARC spit cut off the sediment supply to the Aiguillon spit. On the 1727 CE map the position of the Aiguillon spit was located about 2 km inland compared to ARC spit terminus on the 1755 CE map (Masse map).

In addition, the two recent historical maps from 1909 and 1923 CE show substantial changes in the morphology of the ARC spit over the last centuries. A small sandy spit (called the 'Belle Henriette' spit) appeared from 1909 CE, upstream, in front of the initial root (proximal end) of the ARC spit (Figure 1F,G). This spit elongated rapidly, sheltering the Belle Henriette lagoon (Musereau, 2009). The lagoon remained active until 1972 CE when its outlet was artificially closed. During the stormy winter of 2013/14 CE the outlet was re-opened due to several overwash events (Lashley et al., 2019).

4.2 | Internal architecture, sedimentary constitution and chronology

4.2.1 | The PDB spit

Fruergaard et al. (2020) have provided a description of the architecture of the PDB spit based on the GPR data. On the basis of one GPR profile, the main characteristics of the spit architecture can be summarised as follows: The spit is made up of three main radar units (Figure 4A) between mean and high sea level (section imaged by radar waves). The basal unit is mainly composed of flat reflections, passing locally to inclined reflections featuring

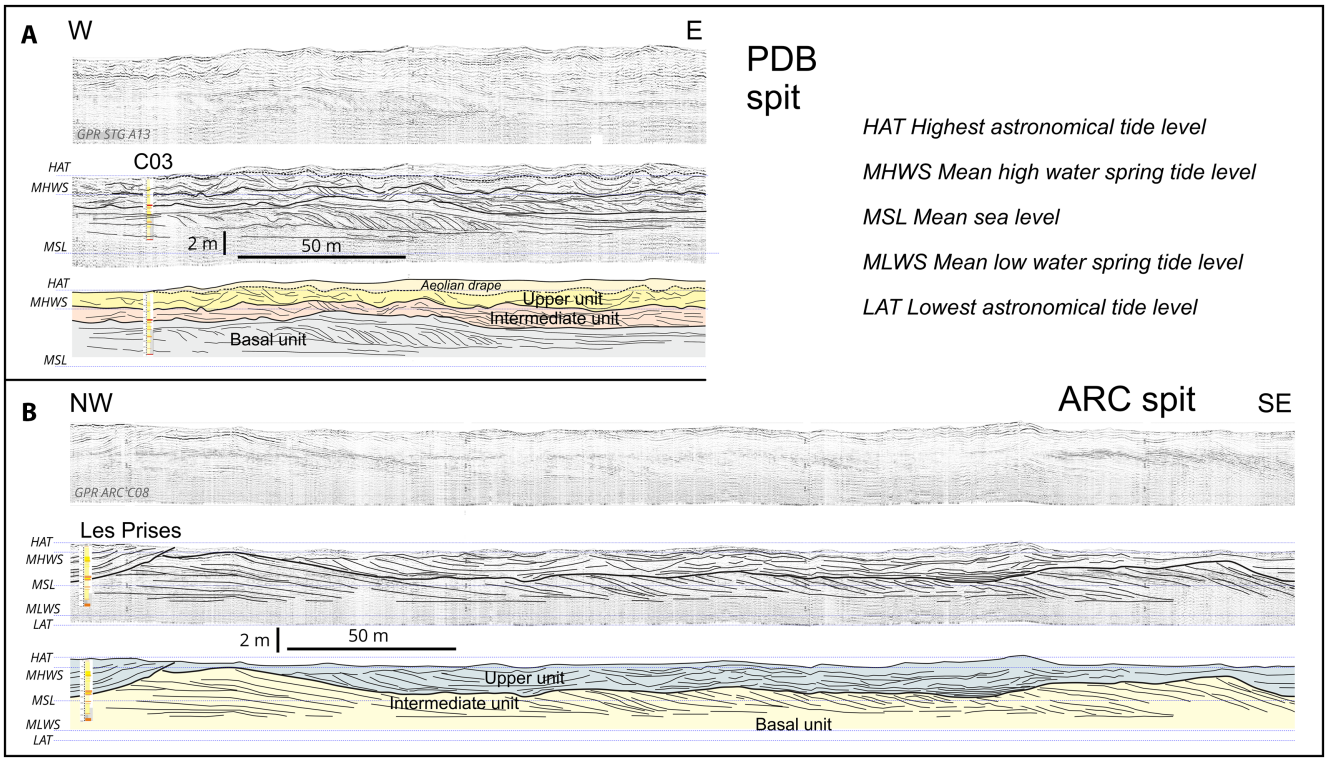

FIGURE 4 Extracts of GRP line collected on the PDB spit (A) and the ARC spit (B). Top, raw GPR line; middle: GPR line with radar reflexion underlined; bottom: GPR line interpretation in terms of radar units (see text for explanation). Location of lines and cores on Figure 2.

landward dips. The intermediate unit overlays the basal unit through semi-continuous and high-intensity reflections. This unit contains discontinuous reflections, locally displaying channelled shape. Landward dipping reflections are visible. Laterally to the west (seaward), reflections gradually flatten. The upper unit rests on the intermediate unit through an erosional surface, which locally deeply cuts the underlying reflections. This top unit contains channelised to wavy reflections, and numerous internal erosional surfaces.

The collected cores show a range of facies extending from fine-grained to very coarse-grained, and well-sorted to very poorly sorted, bioclastic sands (Figure 5A). All cores contain several shelly layers and gravel layers are also present. Sands in the upper part of the cores are generally finer and better sorted. In addition, peat layers are

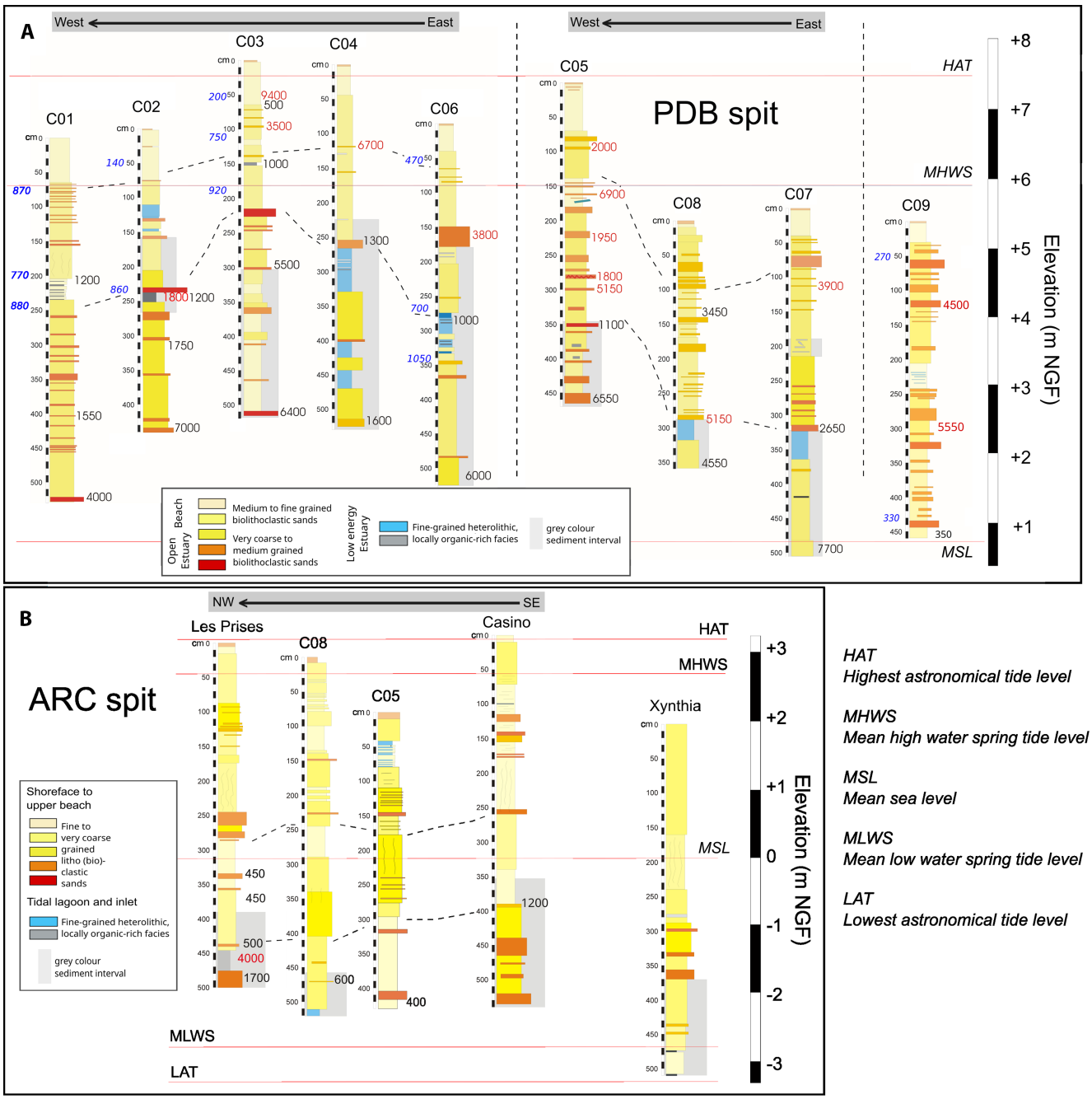

FIGURE 5 Simplified description and environmental interpretation of the sediment cores collected in the PDB spit (A) and the ARC spit (B), with ages. On the left side of the cores in blue italics, mean OSL ages (yr BP, 2σ interval); on the right side of the cores, mean ^{14}C ages (cal. yr. BP, 2σ interval), in red, age inversion. PDB spit ages in Fruergaard et al. (2020); ARC spit ages partly in Poirier et al. (2017a). Dotted lines roughly delineate sedimentary units as defined on the GPR lines (basal, intermediate, upper units). Distance between cores not to scale (see Figure 2 for location, and Figure 6 for more accurate scale).

also preserved, as well as heterolithic sand and clayey facies intervals. In terms of environmental interpretation, finer grained, locally organic-rich facies are interpreted as middle to upper intertidal, or even supratidal, deposits. Moderately to poorly sorted sandy and shelly facies are interpreted as high energy tidal facies (tidal flats and estuary mouth), whereas well-sorted sands are related to beach facies (Fruergaard et al., 2020).

Based on sediment core interpretation and architecture data, the three GPR units are interpreted as follows: The basal and intermediate units correspond to beach or open tidal flat evolving eastward to more or less enclosed estuarine deposits. The landward migrating body within the intermediate unit is interpreted as tidal dunes or swash bars (Fruergaard et al., 2020). The top unit represents the spit unit itself, that is, upper beach deposits, locally with channels formed by barrier breaches, and probably preserved foredune bodies. Note that on the radar profile displayed at Figure 4A, a fourth topmost unit is drawn. It corresponds to the aeolian sand unit, which drapes the entire spit.

The ^{14}C ages cover a large period of time with the maximum age of the spit reaching about 9200 years BP (Poz-65 864), while only two samples (Poz-66 085 and Poz-61 095) coincide with the LIA (upper core C03 and lower core C09). Similar peat layers observed in four cores provide ages corresponding to the beginning of the 8th and 9th centuries and the beginning of the 11th century (Poz-61 510, Poz-6151, Poz-61 513 and Poz-61 514). Several chronological inversions are present in the radiocarbon dataset (ages indicated in red on Figure 5A), which indicate intense sedimentary reworking. The OSL ages support the ^{14}C chronology, if age inversions are excluded.

4.2.2 | The ARC spit

The GPR data collected in the Belle Henriette sector of the ARC spit area image the architecture that corresponds to the spit development during the 17th to 18th century as determined from the historical map analysis. Part of these data are briefly described in Poirier et al. (2017a). The GPR data show that between the low tide and high tide levels (section imaged by GPR data), the spit succession consists of three main units (Figure 4B). The basal unit mainly contains planar reflections. The unit is overlain by a conspicuous unit that clearly delineates a migrating sedimentary body with reflections dipping towards the southeast. The upper unit overlays the migrating unit through an erosional surface that locally deeply incised the unit below. This upper unit displays numerous internal erosional surfaces with wavy geometries.

The five cores retrieved from the ARC spit reveal little variation in the sedimentary facies (Figure 5B). Four cores were collected in the Belle Henriette area, to access the oldest parts of the spit. A fifth core was taken close to the breach created by the Xynthia storm in 2010, to have an analogue in terms of the impact an extreme event can have on the sedimentary signature. Most of the sedimentary facies are fine-grained to coarse-grained lithoclastic to lithobioclastic sands. Few physical structures are observed and the sand appears massive in the cores. Bioclastic particles are observed scattered and rarely arranged in distinct layers. Whole shells are rare. Several of the coarse-grained layers contain gravel. All the deposits are interpreted as low-energy to high-energy beach facies. Only the interval of fine-grained sand with clay drapes that is observed in the upper part of core C05, is interpreted as tide-influenced lagoon facies. Based on sediment core interpretation and architecture data, the three GPR units are interpreted as follows: the basal unit is interpreted as the spit platform (Allard et al., 2008) over which the spit unit itself develops. Above, the top unit represents the uppermost beach, breach infill and washover sediments deposited at the spit during storm wave action, as well as tidal-channel cut and fill deposits which accumulated through migrating channels eroding the landward coast of the spit.

The ^{14}C ages obtained from the ARC cores are consistent with historical maps, which suggest the appearance of the sand spit during the LIA, with five calibrated ages (over eight dated samples) having a 2σ age range from 550 to 370 years BP, corresponding to between 1400 and 1580 AD. Note that there is only one age reversal of the eight ages obtained.

5 | DISCUSSION

5.1 | Comparison of the spit coastline evolution

Historical maps indicate that the ARC spit formed and developed, more or less regularly, since the end of the 17th century. The PDB spit shows a morphology similar to the modern one since the middle of the 18th century. Before this century, the evolution of the area is more difficult to trace due to a lack of reliable cartographic evidence. However, maps from the 16th and beginning of the 17th centuries show a wide estuarine entrance. In contrast, the map of 1689 CE shows a more restricted mouth morphology, indicating that the PDB spit started to develop during the second half of the 17th century. The construction of the entire PDB spit thus occurred between 1650 and 1775 CE and the position of the coastline appears to have been relatively stable in time since then. This is unlike the ARC spit, which has continuously evolved in a longshore direction until today.

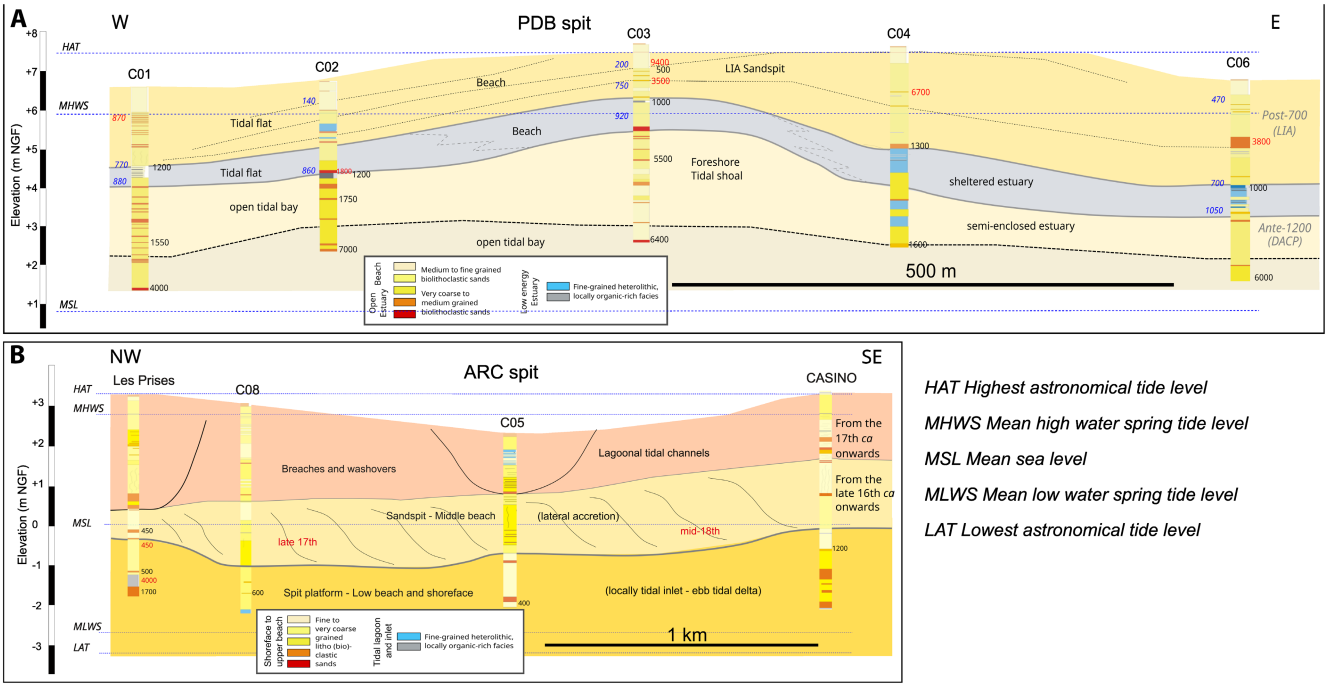

FIGURE 6 Reconstruction of the chronostratigraphy of the PDB spit (A) and ARC spit (B) based on GPR, core, age and coastline evolution data. On the basis of ages and facies evolution provided by cores collected in the PDB spit sediment wedge, the enhanced storm Dark Ages Cold Period (DACP, Helama et al., 2017) is thought to be recorded below the PDB spit that developed after 700 yr BP, probably in relation to the stormy and windy conditions of the LIA (Little Ice Age).

5.2 | Comparison of the spit stratigraphy

The GPR data show distinct architectures that reflect the different modes of evolution of the two spits. The PDB spit architecture reveals vertically stacked units, containing numerous internal surfaces of erosion and amalgamated sedimentary bodies. This architecture results from the fast construction of the spit, with a rapid seaward accretion (progradation) of beach face deposits (Fruergaard et al., 2020) that took place under conditions of a large sand supply. The internal architecture of the ARC spit is consistent with a continuous elongation since the formation of the spit. This elongation, due to a dominant southward-directed littoral drift, took place under lateral accretion of steep beach face deposits at the spit terminus. Above the main spit body, the top unit records highly energetic uppermost beach dynamics associated with wave and swell-induced processes occurring along the spit.

5.3 | Stratigraphic reconstruction and comparison

The PDB spit (Figure 6A) appears to have developed in less than 100 years by accretion of upper beach facies overlaying tidal flats (deposition model C in Tamura, 2012). Foredunes grew in width and elevation to 5–0 m above the highest astronomical tide level preventing further breaching during storms and deposition of washover fans. This fast formation may have been the result of both cross-shore and longshore sediment supply. The ARC spit (Figure 6B) was constructed by lateral accretion of middle to upper beach berms and swash bars (deposit model D in Tamura, 2012). The construction was mainly in a longshore direction. The ^{14}C and OSL ages confirm that both spits start to develop after the 16th century (i.e. 450 cal yr BP). The chronology from the PDB spit clearly shows that the spit becomes younger from the east towards the west and thus confirms that the spit prograded in a seaward direction. Ages from the most basal parts of the two spits suggest that spit construction started with the onset of the LIA. This is particularly clear in the case of the ARC spit. Its proximal end was dated to have started forming from the end of the 17th century and overlays beach sand dated to the 15–16th century. As the spit elongates, foredunes did not develop to the same height as at the PDB spit and it was continuously subject to erosion by storm swell waves, and submersion, inducing breaches and washover deposition. The landward side of the spit was eroded by meandering tidal channels present within the back-barrier lagoon. The evolution of the PDB spit is more complex. Sediment facies successions, ages and internal geometry evidence that a first stage of high-energy sandy sedimentation (foreshore and upper beach) initiated around the

9–10th century. The fine-grained facies that overlay this basal sandy unit reflects low-energy conditions that occurred before the development of the PDB spit unit.

5.4 | Factors explaining the differences between the ARC and PDB spits

Although growth of the two spits was initiated after the 16th century, the spits are different in terms of morphology and dynamics of construction. The progradational pattern of evolution of the triangle shaped PDB spit contrasts with the longshore dominant mode of construction of the more elongated ARC spit (Figure 7). The whole construction of the PDB spit most likely occurred in less than 100 years, whereas the construction of the ARC spit is still ongoing. It is suggested that the main factors explaining the evolutionary differences between the two spits was caused by differences in the sediment supply, longshore transport dynamics and accommodation along the coast.

The general windy and stormy conditions of the LIA likely favoured and enhanced sediment supply by strengthening longshore sediment transport and thus triggering spit formation. The ARC and PDB spits are currently subject to comparable moderate wind and wave conditions. The situation was probably similar in previous centuries because local wave conditions in these two regions are for a large part controlled by coastal configurations (very low slope shoreface, offshore bedrock islands sheltering the coast from oceanic swells). In addition, both sites can be severely impacted by extreme storm events such as the Xynthia storm that hit the ARC spit or the Lothar storm along the PDB coast.

One of the main differences between the two sites relates to the tidal range. Maximum tidal range in the area of the ARC spit is 6.5 m, whereas it is 14 m in the PDB spit region. This makes a significant difference in terms of foreshore and/or intertidal flat width, and therefore of effective aeolian fetch at low tide (Figure 7). Although aeolian fluxes depend on several other parameters than the wind fetch (sediment availability and source width, grain size, moisture, beach morphology, time 'windows'; Nordstrom & Jackson, 1992; Jackson & Cooper, 1999; Bauer et al., 2009; Anthony et al., 2009; de Vries et al., 2014; Castelle et al., 2017; He et al., 2022), it is hypothesised that under enhanced windy conditions, such as those that prevailed during the LIA, wind-induced sand transport across beaches and tidal flats was very high within the PDB spit area. Nowadays, it is very common to notice at low tide landward high sand fluxes over the wide tidal flats due to strong and sustained westerlies (i.e. marine winds). This potential for large amounts of sand to be supplied along the hypertidal coast could explain the fast construction of the PDB spit between 1650 and 1750 CE. Wind-induced sand supply at the ARC spit region was probably lower considering the smaller tidal range and thus shorter effective aeolian fetch. Moreover, as prevailing winds blow obliquely with respect to the coastline direction at both study sites, aeolian sand supply over the foreshore was larger along

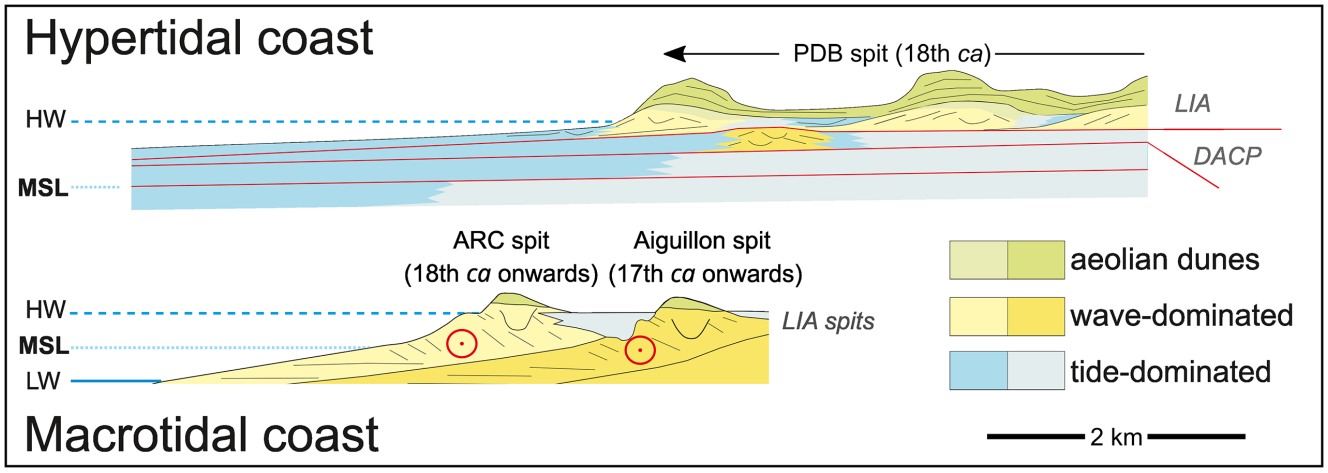

FIGURE 7 Schematic cross-shore sections within the PDB spit and ARC spit. Very wide sandy tidal flats and foreshores due to hypertidal range (14 m) provided a large amount of wind-induced sediment, favouring the fast (in less than one century) and mainly progradational construction of the whole PDB spit. The PDB spit is probably the last stage of edification of a sandy sediment wedge that marks the stormy conditions of the Little Ice Age (LIA), and which succeeds a previous high energy sandy wedge, the ^{14}C ages of which correspond to the Dark Ages Cold Period (DACP). On the macrotidal site (6 m tidal range), due to less wide tidal flats and foreshores, wind-induced sediment supply is supposed to be reduced, while wave-induced longshore transport is highly dominant, resulting in a continuous elongation (red circles) of the ARC spit since the 18th century. The ARC spit is located in front of the earlier Aiguillon spit, both related to the LIA stormy conditions. Bar scale (2 km) for distance estimation. Refer to tidal levels for vertical scale.

the PDB coast compared to the ARC coast. The ARC spit system anchors upstream to a rock-dominated coastline. Such a configuration reduces considerably the regional aeolian fetch. Sediment availability of the PDB spit may also be larger because the spit is part of a much longer continuous sandy coast that constitutes a large sediment reservoir. The spit can, therefore, be sourced by a large amount of sediment from upcoast under certain wind conditions. The timing of low tides is another local factor that controls the 'time windows' (He et al., 2022) for aeolian sand transport. Along the PDB spit coast, low tides during spring tides are around 4 PM, which means that large intertidal areas can dry more easily due to maximum insolation, acting as deflation surfaces potentially during several hours. In comparison, along the ARC spit coast, low tides during spring tides are around noon, and so, early in the afternoon intertidal areas are flooded, shortening the time of wind action on dry sandy surfaces. In addition to probably enhanced wind-induced sand supply at the PBD spit, this site is located close to the inner part of a large-scale embayment bounded by two protruding rocky capes (Figure 2A). At the rocky capes, the coast-normal is oriented towards the south-west and north-west, respectively, whereas at the PDB spit, the coast-normal is approximately oriented towards the west. With dominant westerly winds, waves will approach the shore obliquely at the rocky capes, which generates a longshore sediment transport that is directed towards the south and north, respectively, and that decreases towards the PDB spit. This negative sediment-transport gradient towards the PDB spit contributes to a positive sediment budget at the spit (Fruergaard et al., 2020).

It is assumed that large amounts of wind-induced sediment supply favoured by hypertidal conditions was a key control of the fast construction of the PDB spit. Due to the lower tidal range at the ARC spit, it is suggested that aeolian sediment supply was smaller. On the other hand, although average wave energy can be considered comparable along the PDB and ARC spit coasts, the wave angle at breaking reaches up to 35° along the ARC spit, inducing an important longshore sediment transport, estimated to be about 100,000 m^3 $year^{-1}$ (Bertin et al., 2007). No values are available along the PDB spit, but along the Agon spit, located 25 km further to the south the longshore sediment transport was estimated to be 40,000 m^3 $year^{-1}$ (Robin et al., 2020). This difference partly explains why continuous and active elongation is the main pattern of evolution of the ARC spit since the onset of its construction. This dominant longshore growth is even more accentuated considering that the spit developed with reduced accommodation, along the Aiguillon spit that developed prior to the ARC spit (Figures 3 and 7). In addition, waves at the ARC spit almost always come from one direction causing a unidirectional longshore sediment transport towards the south. At the PDB spit waves can approach the coast both from the north-west and south-west which generates longshore currents from opposite directions. The net longshore drift at the PDB spit will thus be smaller compared to at the ARC spit.

The low gradient shoreface that characterised both sites, of the order of 0.1%, is a geomorphological factor promoting sediment supply to the beaches. A low gradient shoreface induces increased wave skewness and consequently onshore sediment fluxes through landward-migrating nearshore or swash bars (Anthony & Aagaard, 2020; Fruergaard et al., 2021). It is proposed that at both sites the low gradient of the shorefaces contributed to an overall positive sediment supply for the two spits.

6 | CONCLUSION

The aim of the present study was to compare the genesis and evolution of two sandspits, formed under different macrotidal conditions, in order to evaluate the influence of the tidal context in the development of wave-built sedimentary bodies. Both sandspits appeared at the end of the 17th century, probably related to the stormy and windy conditions prevailing during the LIA. The spits have been subject to similar moderate wave conditions during their evolution. The main difference is the tidal range (macrotidal with 6 m vs. hypertidal with 14 m), as well as the general coastal morphological context, and the wave obliquity.

The sand spit from the hypertidal coast was probably constructed in less than 100 years, between 1650 and 1750 CE, as a result of a longshore and mainly progradational (cross-shore) component. The sandspit along the macrotidal site started to develop in the 1700's and continues to grow under the influence of obliquely incoming waves that generate an active longshore sediment transport.

It is proposed that the fast construction of the hypertidal spit is partly due to the large amount of wind-induced sediment supply resulting from the wide intertidal flats and foreshores and consequently a long wind-fetch. Along the macrotidal spit, wind-induced sediment supply is thought to be smaller, but longshore sediment transport is larger and more unidirectional, allowing continuous spit elongation.

The present comparison shows that the evolution of the PDB and ARC spits follows a comparable overall pattern. Differences in relative strength of controlling depositional

mechanisms appear to have caused notable changes in sediment supply to the two spits, resulting in stratigraphic and architectural deviations. It is, however, difficult to determine the relative importance of the complex set of mechanisms that controlled sediment fluxes to the spits. Tidal range is certainly an important parameter, by controlling the amount of aeolian sourced sediment and thus of sand supply to the spits, but large-scale topography of the coastline, cross-shore and longshore sediment supply should be considered as well. Further studies, including previous work reviews, should be performed at large spatial scales, for instance those of the north-western European coasts, in order to determine whether direct relationships between tidal range and wind-induced sediment supply to the foreshore are common, and should consequently be considered to better understand coastal barrier behaviour.

ACKNOWLEDGEMENTS

This work is a contribution to the BLiNiS research project (2013–2014, PI B. Tessier, LITEAU programme). Financial support, including C. Poirier post-doctoral grant, was provided by the French Ministry of Environment (Ministère de l'Ecologie, du Développement Durable et de l'Energie, MEDDE) through the LITEAU funding scheme. M.Fruergaard received funding from Carlsberg Foundation, Denmark (COASTEVENT; grant nos. CF14-0173 and CF15-0254). We warmly thank F. Lelong and S. Haquin from M2C Lab for managing and performing the vibracoring campaigns on both sites. We are grateful to Dr. Cornel Olariu and an anonymous reviewer for their careful and constructive reviews, which contributed to improve the manuscript. We also thank Peter Swart, the editor of the journal, for his kind assistance and helpful advice in improving the latest version of the article. Finally, we express all our thanks to Drs. Sergio Longhitano and Domenico Chiarella, the co-organisers of the Tidalites 2022 conference in Matera and co-editors of this Tidalites 2022 Special Issue in The Depositional Records.

CONFLICT OF INTEREST STATEMENT

The authors declare that they have no known competing financial interests or personal relationships that could have appeared to influence the work reported in this paper.

DATA AVAILABILITY STATEMENT

Data sharing is not applicable to this article.

ORCID

Bernadette Tessier https://orcid.org/0000-0002-1374-7475
Clément Poirier https://orcid.org/0000-0002-8311-8463
Mikkel Fruergaard https://orcid.org/0000-0002-8575-157X
Eric Chaumillon https://orcid.org/0000-0003-1823-7834
Pierre Weill https://orcid.org/0000-0002-6201-1472
Xavier Bertin https://orcid.org/0000-0001-6448-1841
Dominique Mouazé https://orcid.org/0000-0002-6667-4935

REFERENCES

Allard, J. (2008) Enregistrements des changements environnementaux dans les sédiments littoraux: cas des Pertuis Charentais et du Bassin d'Arcachon. Thèse de doctorat, Université de La Rochelle, 284 pp.

Allard, J., Bertin, X., Chaumillon, E. & Pouget, F. (2008) Spit rhythmic development: a potential record of wave climate variations? Arçay Spit, western coast of France. *Marine Geology*, 253, 107–131.

Allard, J., Chaumillon, E. & Féniès, H. (2009) Morphological evolution and stratigraphical record of the progressive closure of a wave-dominated estuary: the Arcachon Lagoon, SW France. *Continental Shelf Research*, 29, 957–969.

Anthony, E.J. & Aagaard, T. (2020) The lower shoreface: morphodynamics and sediment connectivity with the upper shoreface and beach. *Earth-Science Reviews*, 210, 103334.

Anthony, E.J., Ruz, M.H. & Vanhée, S. (2009) Aeolian sand transport over complex intertidal bar-trough beach topography. *Geomorphology*, 105(1–2), 95–105.

Archer, A.W. (2013) World's highest tides: hypertidal coastal systems in North America, South America and Europe. *Sedimentary Geology*, 284, 1–25.

Auphan, E. & Verger, F. (1969) La formation et l'évolution géomorphologique de la Pointe d'Arçay. *Annales du centre régional de documentation pédagogique de Poitiers*, 64–67.

Bauer, B.O., Davidson-Arnott, R.G.D., Hesp, P.A., Namikas, S.L., Ollerhead, J. & Walker, I.J. (2009) Aeolian sediment transport on a beach: surface moisture, wind fetch, and mean transport. *Geomorphology*, 105, 106–116.

Beigbeder, Y. & Verger, F. (1967) Essai de cartographie de La géomorphologie dynamique de la pointe d'Arçay en Vendée. *Revue de Géographie Physique et de Géologie Dynamique*, 9(5), 409–414.

Bertin, X., Deshouilieres, A., Allard, J. & Chaumillon, E. (2007) A new fluorescent tracer experiment improves understanding sediment dynamics of the Arcay sandspit (France). *Geo-Marine Letters*, 27, 63–69.

Bertin, X., Castelle, B., Chaumillon, E., Butel, R. & Quique, R. (2008) Estimation and inter-annual variability of the longshore transport at a high-energy dissipative beach: the St Trojan beach, SW Oléron Island, France. *Continental Shelf Research*, 28, 1316–1332.

Bertin, X., Prouteau, E. & Letetrel, C. (2013) A significant increase in wave height in the North Atlantic Ocean over the 20th century. *Global and Planetary Change*, 106, 77–83.

Bertin, X., Li, K., Roland, A., Zhang, Y.J., Breilh, J.F. & Chaumillon, E. (2014) A modeling-based analysis of the flooding associated with Xynthia, central Bay of Biscay. *Coastal Engineering*, 94, 80–89.

Billeaud, I., Tessier, B. & Lesueur, P. (2009) Impacts of Late Holocene rapid climate changes as recorded in a macrotidal coastal setting (Mont-Saint-Michel Bay, France). *Geology*, 37, 1031–1034.

Castelle, B., Bujan, S., Ferreira, S. & Dodet, G. (2017) Foredune morphological changes and beach recovery from the extreme 2013/2014 winter at a high-energy sandy coast. *Marine Geology*, 385, 41–55.

Chaumillon, E., Proust, J.-N., Menier, D. & Weber, N. (2008) Incised-valley morphologies and sedimentary-fills within the inner shelf of the Bay of Biscay (France): a synthesis. *Journal of Marine Systems*, 72, 383–396.

Chaumillon, E., Bertin, X., Fortunato, A.B., Bajo, M., Schneider, J.L., Dezileau, L., Walsh, J.P., Michelot, A., Chauveau, E., Créach, A., Hénaff, A., Sauzeau, T., Waeles, B., Gervais, B., Jan, G., Baumann, J., Breilh, J.-F. & Pedreros, R. (2017) Storm-induced marine flooding: lessons from a multidisciplinary approach. *Earth-Science Reviews*, 165, 151–184.

Clarke, M.L. & Rendell, H.M. (2011) Atlantic storminess and historical sand drift in Western Europe: implications for future management of coastal dunes. *Journal of Coastal Conservation*, 15, 227–236.

Costas, S., Jerez, S., Trigo, R.M., Goble, R. & Rebêlo, L. (2012) Sand invasion along the Portuguese coast forced by westerly shifts during cold climate events. *Quaternary Science Reviews*, 42, 15–28.

Costas, S., Naughton, F., Goble, R. & Renssen, H. (2016) Windiness spells in SW Europe since the last glacial maximum. *Earth and Planetary Science Letters*, 436, 82–92.

Dashtgard, S.E. & Gingras, M.K. (2007) Tidal controls on the morphology and sedimentology of gravel-dominated deltas and beaches: examples from the megatidal Bay of Fundy, Canada. *Journal of Sedimentary Research*, 77, 1063–1077.

Deat, E. (1995) Morphogenèse et évolution récente de la flèche sableuse et de la lagune de la Belle-Henriette, Propositions de restauration et de gestion du site PNR du Marais Poitevin Val de Sèvre et Vendée. Master thesis, Mémoire de DEA, Université de Brest, 142 p.

de Vries, S., Arens, S.M., De Schipper, M.A. & Ranasinghe, R. (2014) Aeolian sediment transport on a beach with a varying sediment supply. *Aeolian Research*, 15, 235–244.

Dobrynin, M., Murawsky, J. & Yang, S. (2012) Evolution of the global wind wave climate in CMIP5 experiments. *Geophysical Research Letters*, 39, GL052843.

Easterling, D.R., Meehl, G.A., Parmesan, C., Changnon, S.A., Karl, T.R. & Mearns, L.O. (2000) Climate extremes: observations, modeling, and impacts. *Science*, 289, 2068–2074.

Fruergaard, M., Andersen, T.J., Johannessen, P.N., Nielsen, L.H. & Pejrup, M. (2013) Major coastal impact induced by a 1000-year storm event. *Scientific Reports*, 3(1051), 1–7.

Fruergaard, M., Tessier, B., Poirier, C., Mouazé, D., Weill, P. & Noël, S. (2020) Depositional controls on a hypertidal barrier-spit system architecture and evolution, Pointe du Banc spit, northwestern France. *Sedimentology*, 67, 502–533.

Fruergaard, M., Sander, L., Goslin, J. & Andersen, T.J. (2021) Temporary late Holocene barrier-chain deterioration due to insufficient sediment availability, Wadden Sea, Denmark. *Geology*, 49, 162–167.

Galichon, P. (1984) Hydrodynamique sédimentaire des flèches littorales sableuses: cas de la pointe d'Arçay (Vendée). Thèse de docteur ingénieur, Université Paris-Sud, 223 p.

Haslett, S.K., Cundy, A.B., Davies, C.F.C., Powell, E.S. & Croudace, I.W. (2003) Salt marsh sedimentation over the past c. 120 years along the west Cotentin coast of Normandy (France): relationship to sea-level rise and sediment supply. *Journal of Coastal Research*, 19, 609–620.

Hayes, M.O. (1979) Barrier Island morphology as a function of tidal and wave regime. In: Leatherman, S.P. (Ed.) *Barrier Islands*, Vol. 1. New York: Academic Press, p. 27.

Helama, S., Jones, P.D. & Briffa, K.R. (2017) Dark ages cold period: a literature review and directions for future research. *The Holocene*, 27, 1600–1606.

He, Y., Liu, J., Cai, F., Li, B., Qi, H. & Zhao, S. (2022) Aeolian sand transport influenced by tide and beachface morphology. *Geomorphology*, 396, 107987.

Jackson, D. & Cooper, A. (1999) Beach fetch distance and aeolian sediment transport. *Sedimentology*, 46, 517–522.

Jackson, M.G., Oskarsson, N., Tronnes, R.G., McManus, J.F., Oppo, D.W., Grönvold, K., Hart, S.R. & Sachs, J.P. (2005) Holocene loess deposition in Iceland: evidence for millennial-scale atmosphere–ocean coupling in the North Atlantic. *Geology*, 33, 509–512.

Jackson, D.W., Costas, S. & Guisado-Pintado, E. (2019) Large-scale transgressive coastal dune behaviour in Europe during the little ice age. *Global and Planetary Change*, 175, 82–91.

Jelgersma, S., Stive, M.J.F. & van der Valk, L. (1995) Holocene storm signatures in the coastal dunes of western Netherlands. *Marine Geology*, 125, 95–110.

Lashley, C.H., Bertin, X., Roelvink, D. & Arnaud, G. (2019) Contribution of infragravity waves to run-up and overwash in the pertuis breton embayment (France). *Journal of Marine Science and Engineering*, 7, art. no. 205.

Levoy, F., Anthony, E.J., Monfort, O., Robin, N. & Bretel, P. (2013) Formation and migration of transverse bars along a tidal sandy coast deduced from multi-temporal Lidar datasets. *Marine Geology*, 342, 39–52.

Levoy, F., Anthony, E.J., Monfort, O. & Larsonneur, C. (2000) The morphodynamics of megatidal beaches in Normandy, France. *Marine Geology*, 171, 39–59.

Masselink, G. & van Heteren, S. (2014) Response of wave-dominated and mixed-energy barriers to storms. *Marine Geology*, 352, 321–347.

McGranahan, G., Balk, D. & Anderson, B. (2007) The rising tide: assessing the risks of climate change and human settlements in low elevation coastal zones. *Environment and Urbanization*, 19, 17–37.

Menendez, M. & Woodworth, P.L. (2010) Changes in extreme high water levels based on a quasi-global tide-gauge data set. *Journal of Geophysical Research: Oceans*, 115, 100–111.

Miller, G.H., Geirsdottir, A., Zhong, Y., Larsen, D.J., Otto-Bliesner, B.L., Holland, M.M., Bailey, D.A., Refsnider, K.A., Lehman, S.J., Southon, J.R., Anderson, C., Björnsson, H. & Thordarson, T. (2012) Abrupt onset of the Little Ice Age triggered by volcanism and sustained by sea-ice/ocean feedbacks. *Geophysical Research Letters*, 39, GL050168.

Montes, A., Bujalesky, G.G. & Paredes, J.M. (2018) Geomorphology and internal architecture of Holocene sandy-gravel beach ridge plain and barrier spits at Río Chico area, Tierra del Fuego, Argentina. *Journal of South American Earth Sciences*, 84, 172–183.

Montreuil, A.-L., Levoy, F., Bretel, P. & Anthony, E.J. (2014) Morphological diversity and complex sediment recirculation on the ebb delta of a macrotidal inlet (Normandy, France): a multiple LiDAR dataset approach. *Geomorphology*, 219, 114–125.

Mulhern, J.S., Johnson, C.L. & Martin, J.M. (2017) Is barrier Island morphology a function of tidal and wave regime? *Marine Geology*, 387, 74–84.

Musereau, J. (2009) Approche de la gestion des cordons littoraux: Mise au point et application d'un indice d'érosion (Zone des Pertuis Charentais, France). Thèse de doctorat, Université Rennes 2, 306 p.

Neal, A. & Roberts, C. L. (2000) Applications of ground-penetrating radar (GPR) to sedimentological, geomorphological and geoarchaeological studies in coastal environments. In Pye K., Allen J. R. L. (eds). *Coastal and estuarine environments: sedimentology, geomorphology and geoarcheology*. London: Geological Society, Special Publications, **175**, 139–171.

Nicholls, R.J. & Cazenave, A. (2011) Sea-level rise and its impact on coastal zones. *Science*, 328(5985), 1517–1520.

Nordstrom, K.F. & Jackson, N.L. (1992) Effect of source width and tidal elevation changes on Aeolian transport on an estuarine beach. *Sedimentology*, 39, 769–778.

Oppenheimer, M., Glavovic, B.C., Hinkel, J., van de Wal, R., Magnan, A.K., Abd-Elgawad, A., Cai, R., Cifuentes-Jara, M., DeConto, R.M., Ghosh, T., Hay, J., Isla, F., Marzeion, B., Meyssignac, B. & Sebesvari, Z. (2019) Sea level rise and implications for low-lying islands, coasts and communities. In: Pörtner, H.-O., Roberts, D.C., Masson-Delmotte, V., Zhai, P., Tignor, M., Poloczanska, E., Mintenbeck, K., Alegría, A., Nicolai, M., Okem, A., Petzold, J., Rama, B. & Weyer, N.M. (Eds.) *IPCC Special Report on the Ocean and Cryosphere in a Changing Climate*. Cambridge, UK and New York, NY: Cambridge University Press, pp. 321–445.

Pancrazzi, L., Weill, P., Tessier, B., Le Bot, S. & Benoit, L. (2022) Morphostratigraphy of an active mixed sand–gravel barrier spit (Baie de Somme, Northern France). *Sedimentology*, 69, 2753–2778.

Poirier, C., Sauriau, P.-G., Chaumillon, E. & Bertin, X. (2010) Influence ofhydro-sedimentary factors on mollusc death assemblages in a temperate mixed tide-and-wave dominated coastal environment: implications for the fossil record. *Continental Shelf Research*, 30, 1876–1890.

Poirier, C., Tessier, B. & Chaumillon, E. (2017a) Climate control on late Holocene high-energy sedimentation along coasts of the northeastern Atlantic Ocean. *Palaeogeography, Palaeoclimatology, Palaeoecology*, 485, 784–797.

Poirier, C., Tessier, B., Chaumillon, É., Bertin, X., Fruergaard, M., Mouazé, D., Noël, S., Weill, P. & Wöppelmann, G. (2017b) Decadal changes in North Atlantic atmospheric circulation patterns recorded by sand spits since 1800 CE. *Geomorphology*, 281, 1–12.

Poirier, C., Sauzeau, T., Chaumillon, E. & Tessier, B. (2020) Spatially explicit bathymetric reconstruction from lead line depth soundings of the late 17th century. *Estuarine, Coastal and Shelf Science*, 246, 107029.

Robin, N. & Levoy, F. (2007) Etapes et rythmes de formation d'une flèche sédimentaire à crochets multiples en environnement mégatidal. *Zeitschrift für Geomorphologie*, 51, 337–360.

Robin, N., Levoy, F. & Monfort, O. (2009a) Short term morphodynamics of an intertidal bar on megatidal ebb delta. *Marine Geology*, 260, 102–120.

Robin, N., Levoy, F., Monfort, O. & Anthony, E.J. (2009b) Short-term to decadal-scale onshore bar migration and shoreline changes in the vicinity of a megatidal ebb delta. *Journal of Geophysical Research*, 114, F04024.

Robin, N., Levoy, F. & Montfort, O. (2007) Bar morphodynamic behaviour on the ebb delta of a macrotidal inlet (Normandy, France). *Journal of Coastal Research*, 23, 1370–1378.

Robin, N., Levoy, F., Anthony, E.J. & Monfort, O. (2020) Sand spit dynamics in a large tidal-range environment: insight from multiple LiDAR, UAV and hydrodynamic measurements on multiple spit hook development, breaching, reconstruction, and shoreline changes. *Earth Surface Processes and Landforms*, 45, 2706–2726.

Sabatier, P., Dezileau, L., Colin, C., Briqueu, L., Bouchette, F., Martinez, P., Siani, G., Raynal, O. & von Grafenstein, U. (2012) 7000 years of paleostorm activity in the NW Mediterranean Sea in response to Holocene climate events. *Quaternary Research*, 77, 1–11.

Schwartz, M.L. (1982) *The encyclopedia of beaches and coastal environments*. Stroudsburg, PA: Hutchinson Ross Pub. Co., p. 960.

SHOM. (2015) MNT Bathymétrique de façade Atlantique (Projet Homonim). https://doi.org/10.17183/MNT_ATL100m_HOMONIM_WGS84

Sorrel, P., Debret, M., Billeaud, I., Jaccard, S.L., McManus, J.F. & Tessier, B. (2012) Persistent non-solar forcing of Holocene storm dynamics in coastal sedimentary archives. *Nature Geoscience*, 5, 892–896.

Spencer, C.D., Plater, A.J. & Long, A.J. (1998) Rapid coastal change during the mid to late Holocene: the record of barrier estuary sedimentation in the Romney March region, southeast England. *The Holocene*, 8, 143–163.

Stuiver, M. & Reimer, P.J. (1993) Extended C–14 data-base and revised Calib 30 C-14 age calibration program. *Radiocarbon*, 35, 215–230.

Stutz, M.L. & Pilkey, O.H. (2011) Open-ocean barrier islands: global influence of climatic, oceanographic and depositional settings. *Journal of Coastal Research*, 27, 207–222.

Tamura, T. (2012) Beach ridges and prograded beach deposits as paleoenvironment records. *Earth-Science Reviews*, 114, 279–297.

Tessier, B., Delsinne, N. & Sorrel, P. (2010) Holocene sedimentary infilling of a tide-dominated estuarine mouth. The example of the macrotidal Seine estuary (NW France). In: Chaumillon, E., Tessier, B. & Reynaud, J.-Y. (Eds.) *French incised valleys and estuaries*, *Bulletin de la Société Géologique de France*, 181, 87–98.

Tessier, B., Poirier, C., Weill, P., Dezileau, L., Rieux, A., Mouazé, D., Fournier, J. & Bonnot-Courtois, C. (2019) Evolution of a shelly beach ridge system over the last decades in a hypertidal open-coast embayment (western Mont-Saint-Michel Bay, NW France). *Journal of Coastal Research*, 88(SI), 77–88.

Tisnérat-Laborde, N., Paterne, M., Métivier, B., Arnold, M., Yiou, P. & Raynaud, S. (2010) Variability of the northeast Atlantic sea surface $\Delta^{14}C$ and marine reservoir age and the North Atlantic Oscillation (NAO). *Quaternary Science Reviews*, 29, 2633–2646.

Tzanis, A. (2006) MATGPR: a freeware MATLAB package for the analysis of common-offset GPR data. *Geophysical Research Abstracts*, 8, 9488.

van Vliet-Lanoë, B., Goslin, J., Hallégouët, B., Hénaff, A., Delacourt, C., Fernane, A., Franzetti, M., Le Cornec, E., Le Roy, P. & Penaud, A. (2014a) Middle-to late-Holocene storminess in Brittany (NW France): part I–morphological impact and stratigraphical record. *The Holocene*, 24, 413–433.

van Vliet-Lanoë, B., Penaud, A., Hénaff, A., Delacourt, C., Fernane, A., Goslin, J., Hallégouët, B. & Le Cornec, E. (2014b) Middle-to late-Holocene storminess in Brittany (NW France): part II-The chronology of events and climate forcing. *The Holocene*, 24, 434–453.

Vousdoukas, M.I., Voukouvalas, E., Annunziato, A., Giardino, A. & Feyen, L. (2016) Projections of extreme storm surge levels along Europe. *Climate Dynamics*, 47, 3171–3190.

Weill, P. (2010) Formation et évolution de cheniers en contexte macrotidal. Approches expérimentales et in-situ. Thèse de doctorat, Université de Caen Basse Normandie, 282 p.

Weill, P., Tessier, B., Mouazé, D., Bonnot-Courtois, C. & Norgeot, C. (2012) Shelly cheniers on a modern macrotidal flat (Mont-Saint-Michel bay, France)—Internal architecture revealed by ground-penetrating radar. *Sedimentary Geology*, 279, 173–186.

Zazo, C., Dabrio, C.J., Goy, J.L., Lario, J., Cabero, A., Silva, P.G., Bardají, T., Mercier, N., Borja, F. & Roquero, E. (2008) The coastal archives of the last 15 Ka in the Atlantic-Mediterranean Spanish linkage area: sea level and climate changes. *Quaternary International*, 181, 72–87.

Zhang, K. & Leatherman, S. (2011) Barrier Island population along the U.S. Atlantic and Gulf coasts. *Journal of Coastal Research*, 27, 356–363.

How to cite this article: Tessier, B., Poirier, C., Fruergaard, M., Chaumillon, E., Weill, P., Bertin, X. et al. (2024) Role of tidal range and coastline morphology on the evolution of two macrotidal sand spits. *The Depositional Record*, 00, 1–17. Available from: https://doi.org/10.1002/dep2.304